

# VACS equipped vehicles for congestion dissipation in multi-class CTM framework

G. Piacentini<sup>1</sup>, M. Čičić<sup>2</sup>, A. Ferrara<sup>1</sup> and K.H. Johansson<sup>2</sup>

**Abstract**—The advent of connected, automated and autonomous vehicles introduces the possibility for new traffic control approaches. Vehicles equipped with automation and communication systems can be exploited both as sensor and actuators for traffic control actions, thus avoiding the need for new infrastructure. In this paper a multi-class extension of the macroscopic Cell Transmission Model is adopted to describe the interaction between different classes of vehicles, for example human-driven and connected/automated. The vehicle classes are distinguished on the basis of their time headways and their speed. By means of a Model Predictive Control approach, the optimal free-flow speed for the class of connected/automated vehicles is computed and applied to them with the aim of reducing congestion on the highway. The effectiveness of the proposed control law is analyzed depending on the penetration rate of controlled vehicles and the approach is assessed in simulations.

## I. INTRODUCTION

Recent studies on the future of mobility have highlighted that the automotive world is changing fast, thanks to the newly available technology, and in few years the automotive industry will look fundamentally changed. The future of vehicles is expected to move towards four major trends: shared/diverse mobility, electrification, connectivity and autonomous driving [1]. The new mobility system promises to increase customer convenience and safety and to reduce pollutant emissions and congestion levels on highways. To this aim, with the spread of connected, automated and autonomous cars, new traffic control methodologies can be envisaged.

Concerning vehicles automation, there are several intermediate stages that need to be traversed in order to arrive at fully connected and automated mobility, but car connectivity is already a fact. Connectivity allows for new functionalities and features to be offered to drivers and passengers, but also to the traffic management system, with the aim of exploiting smart vehicles for traffic control purposes, both as sensors and as actuators. A connected car is able to exchange information in real time with its surroundings. Several communication systems are currently studied and implemented. Among all the existing VACS (Vehicle Automation and Communication Systems) categories, Vehicle-to-Environment (V2E) communication and, specifically, Vehicle-to-Vehicle (V2V) and Vehicle-to-Infrastructure

(V2I) systems, can be efficiently used for traffic control [2]. These technologies enable data-enhanced driving functionalities, among which is automatic vehicle speed adjustment in accordance with traffic flow and speed limits. Vehicles with automated systems offer to the drivers several functionalities aiming to make the driving experience more safe and efficient. Some of the offered capabilities are autonomous driving on highways, temporary platooning of multiple cars, parking assistance etc. Autonomy allows the vehicle to complete tasks even without the driver being alert, awake or even present. The international standard reported in [3] identifies six levels of automation, starting from level 0, with no automation, to level 5, where a complete automation is present and the human control is no longer necessary and, in many cases, no longer possible. The first question that may arise is what is the penetration rate of connected, automated and autonomous vehicles we should expect in next future. To answer this question, it is interesting to look at the analysis of customer demand about connectivity and automation. Approximately 175 million new connected cars are forecast to be sold globally between 2016 and 2020 and the totality of new cars are expected to be connected by 2025 [4]. Regarding autonomous vehicles, the analysis conducted in [5] reports that fully autonomous vehicles are unlikely to be commercially available before 2030. On the other hand, the portion of vehicles equipped with advanced driver-assistance systems (ADAS) is growing by 23% annually. According to an aggressive scenario envisioned in [5], approximately 50% of passenger vehicles sold in 2030 are expected to be highly autonomous, and another 15% are expected to be fully autonomous. Considering the previous spread forecast, traffic scenarios with high penetration rate of connected/automated vehicles become realistic to be considered. The opportunities introduced to the traffic control and management are substantial. Traffic conditions can now be gathered by means of in-car sensors, in addition to traditional sensors and infrastructure. Optimal speed, time and space headway, lane-changing suggestion can be computed by a central Decision Maker (DM) and communicated to connected cars drivers, or directly actuated as in-driven commands to autonomous cars. A great advantage of traffic control techniques that exploit smart cars features is that no additional infrastructure such as traffic lights and variable speed limit signs are needed, thus leading to cost reduction. Additionally, since these controls are directly communicated to vehicles, we can expect much higher compliance rates than in case of human drivers. A lot of work has been done in the direction of exploiting Connected and Automated Vehicles (CAVs) for traffic control

<sup>1</sup>G. Piacentini, A. Ferrara are with the Department of Electrical, Computer and Biomedical Engineering, University of Pavia, Italy. giulia.piacentini02@universitadipavia.it, antonella.ferrara@unipv.it

<sup>2</sup>M. Čičić, K.H. Johansson are with the Department of Automatic Control, KTH Royal Institute of Technology, Stockholm, Sweden. cicic@kth.se, kallej@kth.se

purposes. This studies are usually carried out by means of microsimulations, see, among others, [6], [7], [8], [9] and [10]. Some recent studies have macroscopically modeled the presence of connected/automated vehicles as moving bottlenecks in the traffic flow, see [11], [12], [13].

In this work, a multi-class extension of the Cell Transmission Model (*CTM*) is used to model a mixed flow of normal human-driven vehicles and automated vehicles. A similar multi-class *CTM* for shared human and autonomous vehicle roads was proposed in [14]. The model presented in this paper is inspired by [15] and [16] where proportional priority is allocated to each class of vehicles. The free-flow speed of the automated vehicles class is taken as control variable to minimize the congestion along the highway. By controlling the connected/automated vehicles, we are also able to indirectly impose a desired speed on the human-driven vehicles. The control problem is formulated in terms of an optimization one and solved by means of a Model Predictive Control (MPC) approach in order to deal with model non-linearities and constraints.

Section II gives a brief account about the *CTM* and describes its multi-class extension, section III formulates the control problem and describes the MPC control approach adopted to solve congestion. Section IV shows the simulations results and reports an analysis of the effectiveness of the controller depending on the penetration rate of CAVs.

## II. MULTI-CLASS CTM

The *CTM* [17] is a first order macroscopic traffic model discrete in both time and space. We consider a road stretch with no on- and off-ramps, divided into  $N$  cells of length  $L$  [km] and a time horizon divided in  $K$  time steps of duration  $T$  [h]. The adopted aggregate variables are:

- $\rho_i(k)$ , the traffic density of cell  $i$  at time step  $k$  [veh/km];
- $\phi_i(k)$ , the traffic flow entering cell  $i$  from cell  $i-1$  during time interval  $[kT, (k+1)T)$  [veh/h];

and the dynamic evolution of the traffic density is given by

$$\rho_i(k+1) = \rho_i(k) + \frac{T}{L} [\phi_i(k) - \phi_{i+1}(k)] \quad (1)$$

The traffic flow leaving cell  $i-1$  is given by the minimum of the so called *demand* from cell  $i-1$ , i.e. the amount of vehicles that would exit from cell  $i-1$ , and the *supply* of cell  $i$ , i.e. the amount of vehicles that cell  $i$  can accommodate. Then these are given by

$$\phi_i(k) = \min \{D_{i-1}(k), S_i(k)\} \quad (2)$$

$$D_{i-1}(k) = \min \left\{ v_{i-1}^{free}(k) \rho_{i-1}(k), q_{i-1}^{\max} \right\} \quad (3)$$

$$S_i(k) = \min \left\{ w_i (\rho_i^{jam} - \rho_i(k)), q_i^{\max} \right\} \quad (4)$$

where  $\rho_i^{jam}$  is the maximum density. The parameters of each cell are the capacity  $q_i^{max}$ , the free-flow speed  $v_i^{free}$  and the congestion wave speed  $w_i$ . We propose an extension to the *CTM* model in order to consider the presence of different

classes of vehicles,  $c \in C$ , to model a flow of both CAVs and human-driven vehicles. Classes are distinguished on the basis of their headway, i.e. the time distance between traveling vehicles, and their free-flow speed. In general, autonomous vehicles allow shorter headway, since their reaction time is shorter than that of human drivers. Let us start by considering only two classes,  $a$  and  $b$ , where  $a$  represents the class of CAVs and  $b$  the class of "background", i.e. human driven vehicles. Classes have headway  $h_a, h_b$  respectively, while  $H$  is a chosen default headway used to derive the parameters of the cells, as the critical density and the jam density. We denote by  $\rho_i^a(k)$  and  $\rho_i^b(k)$  the densities of class  $a$  and  $b$  in cell  $i$  at the time  $k$ . The effective traffic density  $\bar{\rho}$  is defined by summing the densities of individual classes weighed by their headway

$$\bar{\rho}_i(k) = \sum_{c \in C} \frac{h_c}{H} \rho_i^c(k) \quad (5)$$

and we define the share of aggregate flow by

$$\bar{r}_i^c(k) = \frac{\rho_i^c(k)}{\bar{\rho}_i(k)} \quad (6)$$

The class-specific transition flows  $\phi^c$  of each class  $c \in C$  are defined to be proportional to their share  $\bar{r}^c$  and by assuming that different classes have different free flow speed  $v_c$  we define the demand and supply function specific for each class  $c$

$$D_{i-1}^c(k) = \bar{r}_{i-1}^c(k) \min \{v_{i-1}^c(k) \bar{\rho}_{i-1}(k), q_{i-1}^{max}\} \quad (7)$$

$$S_i^c(k) = \bar{r}_{i-1}^c(k) \min \left\{ (\rho_i^{jam} - \bar{\rho}_i(k)) w_i, q_i^{max} \right\} \quad (8)$$

$$\phi_i^c(k) = \min \{D_{i-1}^c(k), S_i^c(k)\} \quad (9)$$

Then we update the state  $\rho^c$  of each class  $c$  according to

$$\rho_i^c(k+1) = \rho_i^c(k) + \frac{T}{L} [\phi_i^c(k) - \phi_{i+1}^c(k)] \quad (10)$$

The total transition flow is given by

$$\phi_i(k) = \sum_{c \in C} \phi_i^c(k) \quad (11)$$

For each cell  $i$  the penetration rate  $p$  of CAVs at time  $k$  is defined as the ratio between the density of CAVs and the total density

$$p(k) = \frac{\rho_i^a(k)}{\rho_i^a(k) + \rho_i^b(k)} \quad (12)$$

The sketch of the freeway divided in cells is reported in Fig.1

In this model the penetration rate is not an a priori imposed parameter. By selecting the boundary conditions, i.e. the inflow and the the outflow for each class, we broadly define the penetration rate that dynamically varies depending on the system evolution.

Since it has been observed that in the presence of a bottleneck

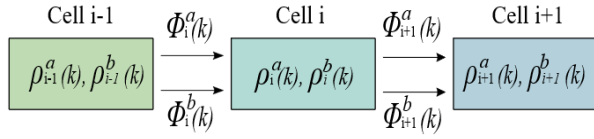


**Fig. 1:** Sketch of the subdivision in cells of the considered stretch of highway.

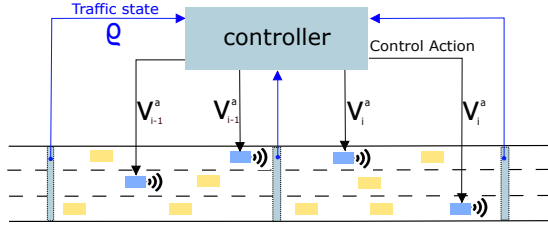


**Fig. 2:** Control scheme.

the discharge flow, i.e. the outflow from the bottleneck, is lower than the capacity of the bottleneck with a reduction around the 5-20 percent and the *CTM* is not able to capture such a phenomena, a further extension has been considered [18]. Among the several extension proposed in literature, here we have chosen to use the one proposed in [19] in which the capacity of each cell is computed as

$$q_i^{\max}(k) = \min \left\{ c_i, c_i \left( 1 - \alpha \frac{\rho_{i-1}(k) - \rho_{i-1}^{cr}}{\rho_{i-1}^{jam} - \rho_{i-1}^{cr}} \right) \right\} \quad (13)$$

where  $c_i$  is the free-flow capacity of cell  $i$  and the parameter  $\alpha$  describes the magnitude of the capacity drop effect.

### III. CONTROL

The control objective of this paper is to avoid, or at least reduce, traffic congestion along the highways. Bottlenecks, i.e. locations with particular characteristics, such as lane-drop, merge areas or temporary events such as traffic accidents, create jams. In this paper, we assume to control the free-flow speed of CAVs, and by controlling them we aim to uniform the traffic density and to reduce the congestion. Fig. 2 depicts the adopted control scheme. The control problem is solved by using a Model Predictive Control approach. At each time step  $k$ , based on the current state information, the controller makes a prediction of the system evolution along the prediction time horizon  $K_p$ . A selected cost function is minimized along the prediction horizon by selecting the optimal control sequence. Only the first sample of the optimal sequence is applied to the system and, at the following time step, based on the new available information, a new prediction is done, according to the receding horizon principle. In this case, the state of the system is given by the density of the two classes  $\rho(k) = [\rho_a(k) \rho_b(k)]$ , while the control variable is the vector of the class  $a$  free-flow speed for each cell  $i = 2, \dots, N$ . The general formulation of the optimization problem over the finite horizon prediction horizon

of  $K_p$  time steps is as follows. At each time step  $k$ , given the current initial state  $\rho(k) = [\rho^a(k) \rho^b(k)]$ , find the optimal control sequence  $\underline{u}(h) = [u_2(h) \dots u_N(h)]$ ,  $h = k, \dots, k + K_p$  that minimizes the objective function  $J$ .  $\underline{u}(h)$  is a matrix having as entries the optimal class  $a$  free-flow speed for every cell  $i = 2, \dots, N$ . Finally, the cost function we consider is given by

$$J = T \sum_{h=k}^{k+K_p} \sum_{i=1}^N L_i \bar{\rho}_i(h) - \beta \sum_{h=k}^{k+K_p} \phi_{i_b}(h) \quad (14)$$

subject to the model dynamics (5)-(13) and to

$$\underline{u}^{\min} \leq \underline{u}(k) \leq \underline{u}^{\max} \quad \text{for } k = 1, \dots, K \quad (15)$$

The first term of the cost function of Eq.(14) represents the Total Travel Time, i.e. the total time spent by all the vehicles along the stretch of highway during the simulated prediction time horizon, while the second term represents the discharge flow from the bottleneck cell  $i_b$  to be maximized and  $\beta$  is its weighting parameter. The non-linear multi-variable minimization problem is solved by means of the interior-point algorithm implemented in the CasADI software tool [20]. The performances of the controller are evaluated by means of the classical congestion indices [21], the Total Travel Time

$$TTT = T \sum_{k=0}^K \sum_{i=1}^N L_i \bar{\rho}_i(k) \quad (16)$$

A second index is the Total Travel Distance (TTD), i.e. the total distance [veh km] covered by all the vehicles in the considered time horizon.

$$TTD = T \sum_{k=0}^K \sum_{i=1}^N L_i \phi_i(k) \quad (17)$$

Where  $\phi_i(k)$  is the total flow leaving cell  $i$  at time step  $k$ . The Mean Speed (MS) [km/h] of the vehicles traveling in the considered system in the whole time horizon is computed as

$$MS = \frac{TTD}{TTT} \quad (18)$$

### IV. SIMULATION RESULTS

The proposed control law is assessed in simulations. To this aim, we consider a scenario with a section of highway composed of  $N = 9$  cells of length  $L_i = 0.7$  [km] for  $i = 1, \dots, N$ . The behavior of each cell is described by a triangular fundamental diagram. The stretch has three lanes, the free-flow capacity of each cell is  $c = 6000$  [veh/h],  $q^{\max}$  is given by Eq.(13), the critical density is  $\rho^{cr} = 63.2$  [veh/km] and the jam density  $\rho^{jam} = 305.1$  [veh/km]. The free-flow speed of the human-driven vehicles class is  $v^b = 95$  [km/h] and the congestion wave speed is  $w = 24.8$  [km/h]. The parameter  $\alpha$  in Eq. (13) expressing the magnitude of the capacity drop phenomenon is equal to 0.56. The time headways have the same value of 1 second for both the classes of vehicles. The overall inflow, i.e. the demand of

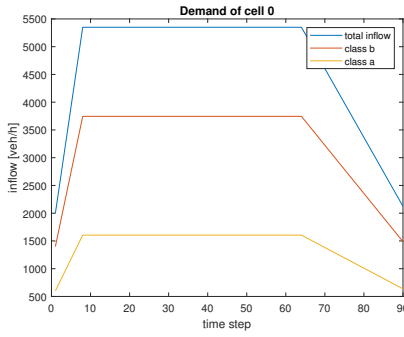


Fig. 3: Demand of cell 0 for class a and b

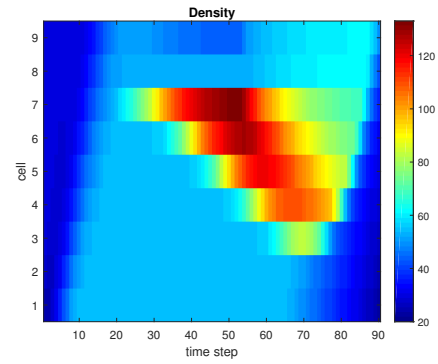
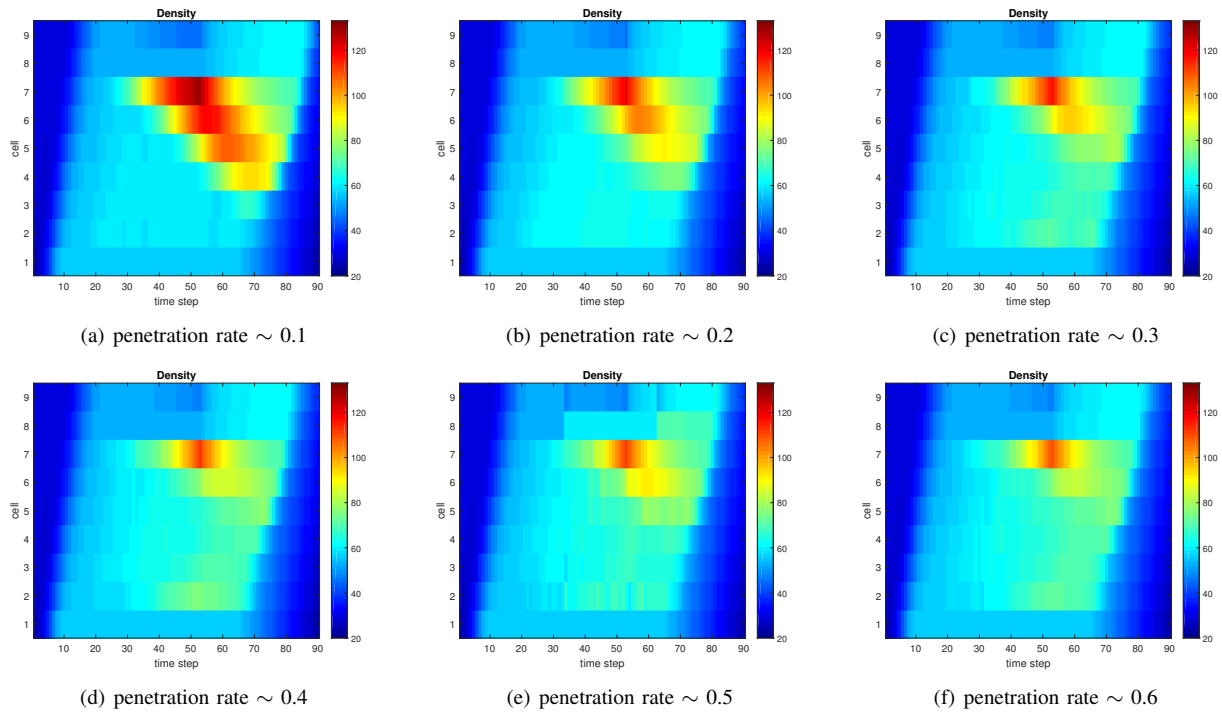


Fig. 4: Density trend in the no-control case

cell 0 given by the sum of the demand of the two classes, has a trapezoidal shape as depicted with the blue line in Fig. 3. The total initial density, given by the sum of the initial density of the two classes, is equal to 30 [veh/km]. A bottleneck is simulated at cell  $i = 8$ , where the free-flow capacity of the cell is reduced to  $c_8 = 5000$  [veh/h] from the beginning of the simulation and it lasts for the 60% of the simulation time, thus simulating the presence of a temporary bottleneck. The free-flow capacity is then restored to its value of 6000 [veh/km]. For the control, the prediction horizon has been chosen  $K_p = 14$  for an overall prediction time of five minutes. The controlled speed is allowed to vary between  $v^{min} = 50$ [km/h] and  $v^{max} = v^{free} = 95$  [km/h]. The control is applied starting from cell  $i = 2$  while no control action is applied to the first cell,  $v_1^a = v^{free}$ . Fig. 4 depicts the behavior of the traffic in the uncontrolled case. In this scenario, the speed of the two classes of vehicles is equal to  $v^{free} = 95$ [km/h] and the model behaves as the classical *CTM* without classes distinction. At time  $k = 7$ , the overall inflow reported in Fig.3 exceeds the value of the capacity of the temporary bottleneck that becomes active and a congestion forms. The congestion propagates upstream, stretching for four cells, due in part to the capacity drop phenomenon limiting the discharge flow from the bottleneck location. With the choice of the parameter  $\alpha = 0.56$ , the maximum capacity drop corresponds to a reduction of the 16%. When the temporary bottleneck is resolved and the capacity of cell  $i = 8$  is restored to the value of 6000 [veh/h], the congestion starts to dissipate. According to (13), the higher the density of cell  $i = 7$ , the higher the reduction of the discharge flow. The control will then aim to avoid the congestion in order to guarantee the maximum discharge rate, thus reducing the capacity drop phenomenon. Fig. 5 depicts the trend of the density in the controlled case depending on the penetration rate of CAVs. The penetration rate is determined by the share of class *a* vehicles present in the inflow but it is not constant along the stretch of road since it varies on the basis of the model dynamics. Even with a low penetration rate of  $\sim 0.1$ , as depicted in Fig. 5(a), there is some mitigation of congestion and a consequent reduction of the travel time. As expected, the higher the penetration rate, the more effective the control action is.

Table I reports the evaluation of the performance indexes introduced in Section III for each penetration rate. The TTT appears to decrease more steeply with penetration rates increasing from 0.1 to 0.3, from the value of 188.79 to 175.22 [veh h], then by further increasing its value, the decrease of the TTT tapers off, thus indicating that over a certain value of penetration rate there is some form of saturation in the control action. The TTD increases as well from the value of 14893 to 14901 [veh km] when  $p = 0.3$ . This causes a consequent increasing of the mean speed. Let us now study in details the scenario in which the penetration rate is  $p = 0.3$ , i.e. the best compromise of lowest penetration rate with good control effectiveness. The inflow for the two class of vehicles is indicated by the orange and yellow line of Fig. 3, while Fig.5(c) shows the trend of the density. The MPC at each iteration computes the optimal velocity for each cell. Fig. 6 reports the trend of the optimal free-flow speed for the class *a* vehicles along the simulation time horizon. The controller tends to properly decrease the speed of the cells that are upstream the temporary bottleneck in order to delay the formation of the traffic jam. The most aggressive control action is applied to cell  $i = 2$ , i.e. the farthest from the bottleneck. The free-flow speed of cell  $i = 9$ , that is located downstream the bottleneck, is kept constant by the controller at the value of 95 [km/h] to guarantee the maximum outflow. Once the temporary bottleneck is cleared the speed is restored at the initial free-flow value of 95 [km/h] for all the cells. Fig. 7 reports the dynamic evolution of the penetration rate. At the beginning of the simulation the penetration rate is constant along the stretch and equal to 0.3 since it is determined only by the inflow. When the control slows down the free-flow speed of the connected/automated vehicles class, they tend to accumulate in the first part of the stretch during the simulation. The accumulation dissolves when the bottleneck is cleared and the automated/connected vehicles class can flow at the free-flow speed of 95 [km/h]. The density trends appears to be globally more uniform along the stretch of highway, the congestion propagates for only one cell upstream the bottleneck and really high value of the density are present only in the cell immediately upstream the bottleneck for a short span of time.



**Fig. 5:** Comparison of the same scenario with different penetration rate

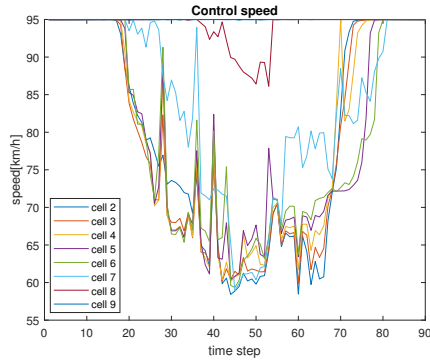


**Fig. 6:** Free-flow speed for class *a* for each cell given by the controller

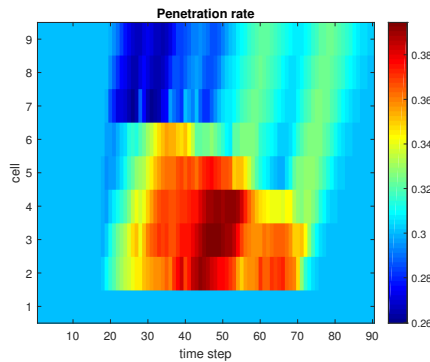


**Fig. 7:** Penetration rate of class *a* vehicles along the stretch of highway

**TABLE I:** Comparison between cost functionals in the uncontrolled case and in the control case with different penetration rate.

	TTT	TTD	MS
No control	188.7947	14893	78.88
$p=0.1$	183.2409	14895	81.29
$p=0.2$	176.8308	14900	84.26
$p=0.3$	175.2191	14901	85.04
$p=0.4$	173.6013	14901	85.84
$p=0.5$	174.7722	14899	85.25
$p=0.6$	173.0361	14903	86.13

## V. CONCLUSIONS

In this paper we have presented a simple way of considering a mixed flow of normal human-driven cars and automated/connected cars from a macroscopic modeling point of view, thus avoiding the high computational burden deriving from microscopic models. By controlling only the speed of the connected/automated class vehicles are also able to influence the human-driven vehicles and obtain benefits for the overall traffic flow. The main purpose of this control has been a density homogenization and a congestion reduction. An analysis of the effectiveness of the control depending on the penetration rate has been done taking into account the expected forecast of connected/automated vehicles market spread. The congestion appears to be globally reduced even with low penetration rate of automated/connected vehicles. The performance indexes of the congestion are all improved by the application of the control action.

## ACKNOWLEDGMENT

The research leading to these results has received funding from the European Union's Horizon 2020 research and innovation programme under the Marie Skłodowska-Curie grant agreement No 674875, VINNOVA within the FFI program under contract 2014-06200, the Swedish Research Council, the Swedish Foundation for Strategic Research and Knut and Alice Wallenberg Foundation. The second author is affiliated with the Wallenberg AI, Autonomous Systems and Software Program (WASP).

## REFERENCES

- [1] D. Wee, M. Kässer, M. Bertoncello, *et al.*, "Competing for the connected customer: Perspectives on the opportunities created by car connectivity and automation", McKinsey&Company, Tech. Rep., 2015.
- [2] C. Diakaki, M. Papageorgiou, I. Papamichail, and I. Nikolos, "Overview and analysis of Vehicle Automation and Communication Systems from a motorway traffic management perspective", *Transportation Research Part A: Policy and Practice*, vol. 75, pp. 147–165, May 2015.
- [3] "J3016: Taxonomy and Definitions for Terms Related to On-Road Motor Vehicle Automated Driving Systems", SAE International, Tech. Rep., 2014, p. 12.
- [4] "Connected Cars global forecast", SBD Automotive, Tech. Rep., 2018.
- [5] B. Heid, C. Huth, S. Kempf, and G. Wu, "Ready for inspection: The automotive aftermarket in 2030", McKinsey&Company, Tech. Rep., 2018.
- [6] C. Roncoli, I. Papamichail, and M. Papageorgiou, "Model Predictive Control for Motorway Traffic with Mixed Manual and VACS-equipped Vehicles", *Transportation Research Procedia*, vol. 10, pp. 452–461, Jan. 2015.
- [7] C. Roncoli, M. Papageorgiou, and I. Papamichail, "Traffic flow optimisation in presence of vehicle automation and communication systems – Part II: Optimal control for multi-lane motorways", *Transportation Research Part C: Emerging Technologies*, vol. 57, pp. 260–275, Aug. 2015.
- [8] E. Grumert, X. Ma, and A. Tapani, "Analysis of a cooperative variable speed limit system using microscopic traffic simulation", *Transportation Research Part C: Emerging Technologies*, vol. 52, pp. 173–186, Mar. 2015.
- [9] X.-Y. Lu and S. E. Shladover, "Mpc-based variable speed limit and its impact on traffic with v2i type acc", in *Proceedings of The 21st IEEE International Conference on Intelligent Transportation Systems, Maui, Hawaii, USA, November 4-7, 2018*.
- [10] E. Vinitzky, K. Parvate, A. R. Kreidieh, *et al.*, "Lagrangian control through deep-rl: Applications to bottleneck decongestion", in *Proceedings of The 21st IEEE International Conference on Intelligent Transportation Systems, Maui, Hawaii, USA, November 4-7, 2018*.
- [11] G. Piacentini, P. Goatin, and A. Ferrara, "Traffic control via moving bottleneck of coordinated vehicles", *Proceedings of 15th IFAC Symposium on Control in Transportation Systems CTS 2018*, vol. 51, no. 9, pp. 13–18, Jan. 2018.
- [12] C. Pasquale, S. Sacone, S. Siri, and A. Ferrara, "New Micro-Macro METANET Model for Platoon Control in Freeway Traffic Networks", in *Proceedings of The 21st IEEE International Conference on Intelligent Transportation Systems, Maui, Hawaii, USA, November 4-7, 2018*.
- [13] M. Čičić and K. H. Johansson, "Traffic regulation via individually controlled automated vehicles: a cell transmission model approach", in *2018 21st International Conference on Intelligent Transportation Systems (ITSC)*, IEEE, Nov. 2018, pp. 766–771.
- [14] M. W. Levin and S. D. Boyles, "A multiclass cell transmission model for shared human and autonomous vehicle roads", *Transportation Research Part C: Emerging Technologies*, vol. 62, pp. 103–116, Jan. 2016.
- [15] M. Wright, G. Gomes, R. Horowitz, and A. A. Kurzhanskiy, "A new model for multi-commodity macroscopic modeling of complex traffic networks", Sep. 2015. arXiv: 1509.04995.
- [16] L. Jin, M. Cicic, S. Amin, and K. H. Johansson, "Modeling Impact of Vehicle Platooning on Highway Congestion: A Fluid Queuing Approach", in *21st ACM International Conference on Hybrid Systems: Computation and Control (HSCC)*, 2018.
- [17] C. F. Daganzo, "The cell transmission model: A dynamic representation of highway traffic consistent with the hydrodynamic theory", *Transportation Research Part B: Methodological*, vol. 28, no. 4, pp. 269–287, Aug. 1994.
- [18] M. Kontorinaki, A. Spiliopoulou, C. Roncoli, and M. Papageorgiou, "First-order traffic flow models incorporating capacity drop: Overview and real-data validation", *Transportation Research Part B: Methodological*, vol. 106, pp. 52–75, Dec. 2017.
- [19] Y. Han, A. Hegyi, Y. Yuan, *et al.*, "Resolving freeway jam waves by discrete first-order model-based predictive control of variable speed limits", *Transportation Research Part C: Emerging Technologies*, vol. 77, pp. 405–420, Apr. 2017.
- [20] J. A. E. Andersson, J. Gillis, G. Horn, J. B. Rawlings, and M. Diehl, "CasADi – A software framework for nonlinear optimization and optimal control", *Mathematical Programming Computation*, In Press, 2018.
- [21] A. Ferrara, S. Sacone, and S. Siri, "An Overview of Traffic Control Schemes for Freeway Systems", in *Freeway Traffic Modelling and Control*, Springer, Cham, 2018, ch. 8, pp. 193–234.